ORIGINAL PAPER

CrossMark

Knockdown of STEAP1 inhibits cell growth and induces apoptosis in LNCaP prostate cancer cells counteracting the effect of androgens

Inês Margarida Gomes[1] · Sandra Moreira Rocha[1] · Carlos Gaspar[1] · Maria Inês Alvelos[2] · Cecília Reis Santos[1] · Sílvia Socorro[1] · Cláudio Jorge Maia[1]

Abstract

Six transmembrane epithelial antigen of the prostate 1 (STEAP1) is overexpressed in numerous types of tumors, especially in prostate cancer. STEAP1 is located in the plasma membrane of epithelial cells and may play an important role in inter- and intracellular communication. Several studies suggest STEAP1 as a potential biomarker and an immunotherapeutic target for prostate cancer. However, the role of STEAP1 in cell proliferation and apoptosis remains unclear. Therefore, the role of STEAP1 in prostate cancer cells proliferation and apoptosis was determined by inducing STEAP1 gene knockdown in LNCaP cells. In addition, the effect of DHT on the proliferation of LNCaP cells knocked down for STEAP1 gene was evaluated. Our results demonstrated that silencing the STEAP1 gene reduces LNCaP cell viability and proliferation, while inducing apoptosis. In addition, we showed that the cellular and molecular effects of STEAP1 gene knockdown may be independent of DHT treatment, and blocking STEAP1 may reveal to be an appropriate strategy to activate apoptosis in cancer cells, as well as to prevent the proliferative and anti-apoptotic effects of DHT in prostate cancer.

Keywords STEAP1 · Prostate cancer · siRNA · Apoptosis · Proliferation

Introduction

Prostate cancer (PCa) is the most commonly diagnosed cancer and the second leading cause of cancer-related death in men in the western world [1]. Considered a hormone-dependent cancer, the role of androgens in prostate physiology has been extensively studied showing relevance for the normal prostate development and growth, as well as for PCa development [2, 3].

The six transmembrane epithelial antigen of the prostate 1 (STEAP1) is up-regulated in PCa and, to a less extent, in other types of cancer also [4–10]. Remarkably, STEAP1 expression in normal tissues is almost exclusively restricted to the prostate, making it a very promising biomarker and immunotherapeutic target in cancer [5, 10–16]. STEAP1 is

mainly located at the plasma membrane of epithelial cells, but it can also be found dispersed in the cytoplasm [5, 6, 8, 10]. It has been suggested that STEAP1 may act as an ion channel or transporter protein at the cell–cell junctions in the prostate where it may be involved in intercellular communication [17, 18]. Knowledge on the regulation of STEAP1 expression is still limited. However, it has been demonstrated that zoledronic acid and 17β-estradiol inhibit STEAP1 mRNA expression in PCa cells and in normal breast and breast cancer cells [6, 19]. Unexpectedly, 5α-dihydrotestosterone (DHT) down-regulates STEAP1 expression in LNCaP cells, but considering that the effect of DHT on STEAP1 regulation is not mediated by the androgen receptor, it is plausible that this down-regulation may occur as a result of a negative feedback mechanism in order to overcome the proliferative effects of DHT [8].

Considering that STEAP1 is overexpressed in PCa and several studies have pointed out STEAP1 as an oncoprotein, we aimed to investigate the oncogenic potential of STEAP1. Therefore, we knocked down STEAP1 expression by transfecting LNCaP cells with siRNA and analyzed the effects of STEAP1 silencing in cell proliferation and apoptosis. The effect of DHT in the proliferation of STEAP1 knockdown

✉ Cláudio Jorge Maia
  cmaia@fcsaude.ubi.pt

1 CICS-UBI - Health Sciences Research Centre, University of Beira Interior, Av. Infante D. Henrique, 6200-506 Covilhã, Portugal

2 ULB Center for Diabetes Research, Université Libre de Bruxelles, 1070 Brussels, Belgium

LNCaP cells was also assessed. Herein, we provide evidence that STEAP1 is involved in PCa cell survival, and that its expression may abrogate proliferative and anti-apoptotic effects of DHT.

Materials and methods

Cell culture and STEAP1 knockdown

The LNCaP prostate cancer cell line was purchased from the European Collection of Cell Cultures (ECACC, UK) and maintained in RPMI 1640 medium (Gibco, Scotland) supplemented with 10% fetal bovine serum (FBS) (Biochrom AG, Germany) and 1% penicillin/streptomycin (Invitrogen, USA), in a humidified chamber at 37 °C and a 5% CO_2 atmosphere. LNCaP cells at 40% confluence in six-plate multiwells were transfected with 50 and 100 nM of a small interfering RNA (siRNA) targeting the STEAP1 (s25634) (Ambion, USA) and 5 μL of Lipofectamine 2000 (Invitrogen, USA) for 24 h in Opti-MEM medium (Invitrogen, USA), as recommended by the manufacturer. As a control for STEAP1-specific targeting, a scrambled siRNA sequence (AM4635) was used. The efficiency of STEAP1 knockdown expression was analyzed by quantitative real-time PCR (qPCR). In order to confirm the STEAP1 knockdown at the protein level, LNCaP cells were transfected with 50 nM of siRNA for 24 h, after which the medium was replaced to complete medium. Cells were harvested at 0, 12, 24 and 48 h after transfection, and STEAP1 protein expression was analyzed by Western blot.

DHT treatment of LNCaP cells

After cell transfection with siRNA, the medium was changed to phenol red free RPMI 1640 medium supplemented with 5% charcoal-stripped FBS (CS-FBS) (Gibco, USA), which was replaced after 24 h by fresh CS-FBS, containing 0 nM (control) or 10 nM DHT. Cells were harvested after 48 h and seeded in coverslips for the Ki67 analysis or TUNEL assay. For the MTS assay, prior to hormonal deprivation with CS-FBS, 1×10^3 LNCaP cells were seeded per well in 96-multiwell plates.

Quantitative real-time polymerase chain reaction (qPCR)

Total RNA from LNCaP cells was obtained using TRI reagent (Ambion, UK) according to the manufacturer's instructions. Total RNA integrity and quantification were assessed by agarose electrophoresis and measurement of absorbances at 260 and 280 nm on a nanospectrometer (Pharmacia Biotech, Ultrospec 3000). cDNA was synthesized using the NZY First-Strand cDNA Synthesis Kit (NZYTech, Portugal), in accordance with the manufacturer's protocol.

qPCR was used to determine the expression of STEAP1 and the percentage of STEAP1 gene knockdown. qPCRs were performed on the IQ5 Multicolor qPCR Detection System (Bio-Rad, Hercules, USA) using Maxima™ SYBR Green/Fluorescein qPCR Master Mix (Thermo Scientific, Vilnius, Lithuania). The efficiency of qPCR was determined for all designated primers (Table 1) with serial dilutions (1:1; 1:10; 1:100; 1:1000) of the cDNA. qPCRs were performed using 1 μL of cDNA in a 20-μL reaction containing 10 μL SYBR Green and 300 nM of specific primers. After an initial denaturation at 95 °C for 5 min, 35 cycles were carried out as follows: denaturation at 95 °C for 30 s, annealing temperature for 30 s and polymerization at 72 °C for 20 s. The amplified PCR fragments were analyzed by melting curves: Reactions were heated from 55 to 95 °C with 10-s holds at each temperature (0.05 °C/s). Human glyceraldehyde 3-phosphate dehydrogenase (GAPDH) and beta-2-microglobulin (β2M) were used as internal controls to normalize gene expression. Fold differences were calculated following the mathematical model proposed by Pfaffl [20].

Table 1 Sequences and resulting amplicon sizes of the specific primers and cycling conditions used in qPCR

Oligo name	Sequence (5′–3′)	Amplicon size (bp)	Annealing temperature (°C)
STEAP1	Sense: GGCGATCCTACAGATACAAGTTGC	128	60
	Anti-sense: CCAATCCCACAATTCCCAGAG AC		
p21	Sense: GTTCCTTGCCACTTCTTAC	103	53
	Anti-sense: ACTGCTTCACTGTCATCC		
GAPDH	Sense: 5′CGCCCGCAGCCGACACATC3′	75	60
	Anti-sense: 5′CGCCAATACGACCAAATCCG3′		
2M	Sense: 5′ATGAGTATGCCTGCCGTGTG3′	92	60
	Anti-sense: 5′CAAACCTCCATGATGCTGCTTAC3′		

Western blot

LNCaP cells were lysed on an appropriate volume of RIPA buffer (150 mM NaCl, 1% Nonidet-P40 substitute, 0.5% Na-deoxycholate, 0.1% SDS, 50 mM Tris, 1 mM EDTA) supplemented with 1% protease cocktail and 10% PMSF. The total protein extract was obtained after centrifugation of the cell lysate for 20 min at 12,000 rpm and 4 °C. Quantification of the total protein bulk was measured using the Bradford method (Bio-Rad, USA). Approximately 50 µg of total protein from LNCaP cells was used to determine STEAP1 protein expression as previously described [8]. Briefly, proteins were resolved on 12% SDS-PAGE electrophoresis gel and then transferred into a PVDF membrane (GE Healthcare, UK). After blockage with 3% casein solution, membranes were incubated overnight at 4 °C with rabbit anti-STEAP1 (1:300, H105, sc-25,514, Santa Cruz Biotechnology, CA), rabbit anti-Bax (1:1000, no. 2772, Cell Signaling Technology, MA), rabbit anti-Bcl-2 (1:1000, no. 2876, Cell Signaling Technology, MA), rabbit anti-caspase-9 (1:1000, H-170, sc-8355, Santa Cruz Biotechnology, CA), mouse anti-caspase-8 (1:1000, D-8, sc-5263, Santa Cruz Biotechnology, CA), rabbit anti-p53 (1:1000, FL-393, sc-6243, Santa Cruz Biotechnology, CA), rabbit anti-FasR (1:1000, A-20, sc-1023, Santa Cruz Biotechnology, CA) or rabbit anti-FasL (1:1000, C-178, sc-6237, Santa Cruz Biotechnology, CA). A mouse anti-β-actin (1:1000, A5441, Sigma–Aldrich) was used for the normalization of protein expression. Membranes were incubated with goat anti-rabbit IgG-HRP (1:40,000, sc-2004, Santa Cruz Biotechnology, CA) or goat anti-mouse IgG-HRP (1:40,000, sc-2005, Santa Cruz Biotechnology, CA). Finally, immunoreactivity was visualized using the ChemiDoc™ MP Imaging System (Bio-Rad) after a brief incubation with ECL substrate. Protein expression levels were quantified by densitometry analysis using the Image Lab 5.1 software (Bio-Rad).

MTS assay

The MTS assay (Promega, USA) was used, according to the manufacturer's instructions, to evaluate cell viability. Briefly, 20 µL of MTS solution was added to the 100 µL of culture media at the same time as the medium containing 0 nM or 10 nM DHT. After incubation at 37 °C, the optical density was measured at 490 nm after 24 h and 48 h. Results are presented for absorbance at 490 nm as a function of time.

Ki67 fluorescence immunocytochemistry

LNCaP cells were fixed with 4% PFA and permeabilized with 1% Triton X-100 for 5 min at room temperature. Unspecific staining was blocked by incubation with PBS containing 0.1% (w/v) Tween-20 and 20% FBS (Biochrom AG) for 1 h. Cells were then washed with PBS and incubated for 1 h at RT with rabbit anti-Ki67 (1:50, no. 16667, Abcam). Incubation with the Alexa Fluor 546 goat anti-rabbit IgG secondary antibody (1:500, Invitrogen) was performed for 1 h at RT. Cells were washed in PBS and incubated for 5 min in Hoechst-33342 (Invitrogen, UK) 5 µg/mL. Coverslips were then mounted in Dako (Invitrogen, UK) and analyzed by fluorescence microscopy. Negative controls were performed by the omission of the primary antibody (data not shown). The preparations were observed in a Zeiss inverted microscope (Carl Zeiss). The proliferation index was estimated by counting the number of Ki67-positive cells and Hoechst-stained nuclei in twenty randomly selected 40× magnification fields for each section. The ratio between the number of Ki67-stained cells and total number of nuclei was calculated.

TUNEL assay

Detection and quantification of apoptosis were determined using the in situ cell death detection kit, TMR red (Roche, Germany), in accordance with the manufacturer's instructions. Briefly, cells were washed in PBS, fixed with 4% PFA for 10 min and, then, permeabilized in 1% Triton X-100 for 5 min. Fifty microliters of TUNEL reaction mixture was added to each sample for 1 h at 37 °C in the dark. Cells were washed in PBS and incubated for 5 min in Hoechst-33342 (Invitrogen, UK) 5 µg/mL. Coverslips were then mounted in Dako (Invitrogen, UK) and analyzed by fluorescence microscopy. Negative controls were performed by the omission of the primary antibody (data not shown). The percentage of apoptotic cells was estimated by counting the number of TUNEL-positive cells and Hoechst-stained nuclei in twenty randomly selected 40× magnification fields in each coverslip. The ratio between the number of TUNEL-positive cells and total number was calculated.

Caspase-3 activity assay

The activity of caspase-3 was assessed determining the cleavage of a colorimetric substrate. Briefly, proteins (50 µg) were incubated with a reaction buffer (25 mM HEPES, pH 7.5, 0.1% CHAPS, 10% sucrose and 10 mM DTT) and 100 mM of caspase-3 substrate (Ac-DEVD-pNA) for 2 h at 37 °C. The caspase-3-like activity was determined after the cleavage of the labeled substrate by the detection of the chromophore p-nitroaniline, measured spectrophotometrically at 405 nm. The method was calibrated with known concentrations of p-nitroanilide.

Statistical analysis

Data from all experiences are shown as mean $\pm$ SEM of $n = 3$. The statistical significance of all experiments was

assessed using one-way ANOVA followed by Bonferroni test.
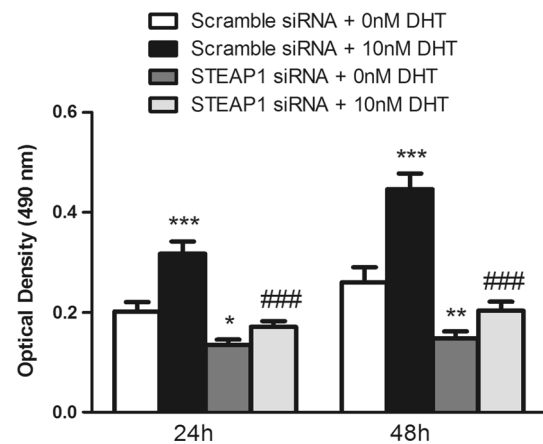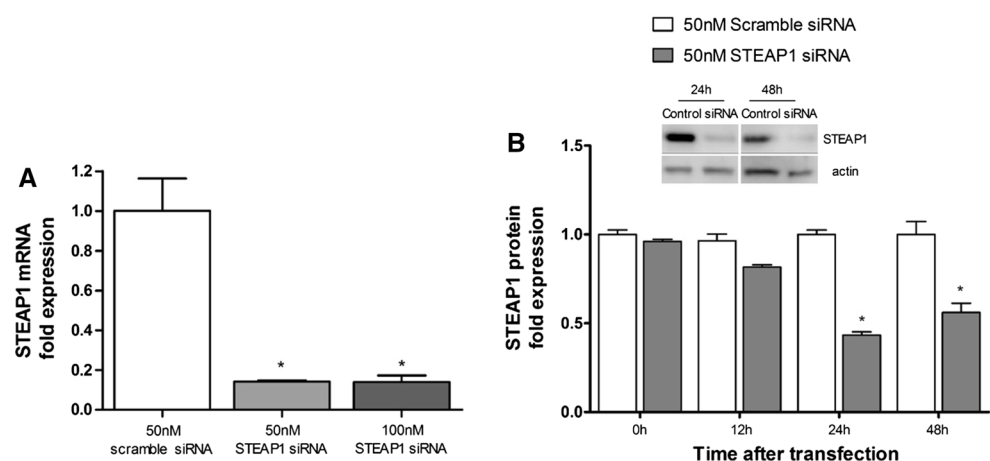
Results

STEAP1 gene knockdown using a specific siRNA

To optimize STEAP1 knockdown, two different doses of siRNA were used to transfect LNCaP cells for 24 h, and the levels of STEAP1 mRNA were determined by qPCR. As shown in Fig. 1a, STEAP1 gene expression was effectively down-regulated (approximately 90%, $p < 0.05$) using 50 nM or 100 nM of STEAP1 siRNA, when compared to control. To determine the time required to observe STEAP1 down-regulation at the protein level, cells were transfected with 50 nM siRNA. Western blot analysis demonstrated that at 24 and 48 h after transfection, STEAP1 expression was reduced by approximately 50% when compared to control (Fig. 1b, $p < 0.05$). For the following experiments, 50 nM STEAP1 siRNA was used and the cellular and molecular effects were evaluated at 24 h and/or 48 h after transfection.

STEAP1 gene knockdown decreases LNCaP cells viability and proliferation and induces apoptosis

Considering that STEAP1 is overexpressed in LNCaP cells, we compared the effect of STEAP1 gene silencing relatively to control cells. As shown in Fig. 2, knockdown of STEAP1 reduced cell viability by approximately 33 and 40% in comparison with control after 24 h ($p < 0.05$) and 48 h ($p < 0.01$). Considering the results obtained with the MTS assay, the next step was to clarify the effect of STEAP1 silencing in cell proliferation and apoptosis using the Ki67 index and TUNEL assay. Cell proliferation index was significantly decreased after STEAP1 gene silencing in LNCaP cells (0.3-fold variation when compared to control, Fig. 3a,

Fig. 2 Analysis of cell viability by means of MTS assay. Error bars indicate mean ± SEM ($n = 12$). *$p < 0.05$. **$p < 0.01$, ***$p < 0.001$ when compared to scramble siRNA + 0 nM DHT-treated cells (control cells); ##$p < 0.01$, ###$p < 0.001$ when compared to scramble siRNA + 10 nM DHT-treated cells; $p < 0.05$, $$$p < 0.01$ when compared to STEAP1 siRNA + 0 nM DHT-treated cells (one-way ANOVA followed by Bonferroni test)

c, e, $p < 0.01$). The STEAP1 knockdown increased the number of TUNEL-stained cells in relation to control (2.2-fold variation, Fig. 3f, h, j, $p < 0.05$).

STEAP1 gene knockdown regulates the expression of cell cycle and apoptosis regulators

To determine the influence of STEAP1 on cell cycle and apoptosis pathways, we assessed the protein levels of key regulators of these processes: p53, p21, Bax, Bcl-2, caspase-9, FasR, FasL, caspase-8 and caspase-3. The knockdown of STEAP1 gene increased the expression of p53 in comparison with the control group (4.7-fold variation, $p < 0.001$, Fig. 4a, b). Also, the p21 mRNA expression was increased in STEAP1 knockdown LNCaP cells (3.0-fold

Fig. 1 Analysis of STEAP1 gene knockdown by qPCR (**a**) and Western blot (**b**). mRNA expression was normalized with hGAPDH and hβ2M, and protein expression was normalized with β-actin. Error bars indicate mean ± SEM ($n = 3$). *$p < 0.05$ (one-way ANOVA followed by Bonferroni test) compared with scramble siRNA + 0 nM DHT-treated cells (control)

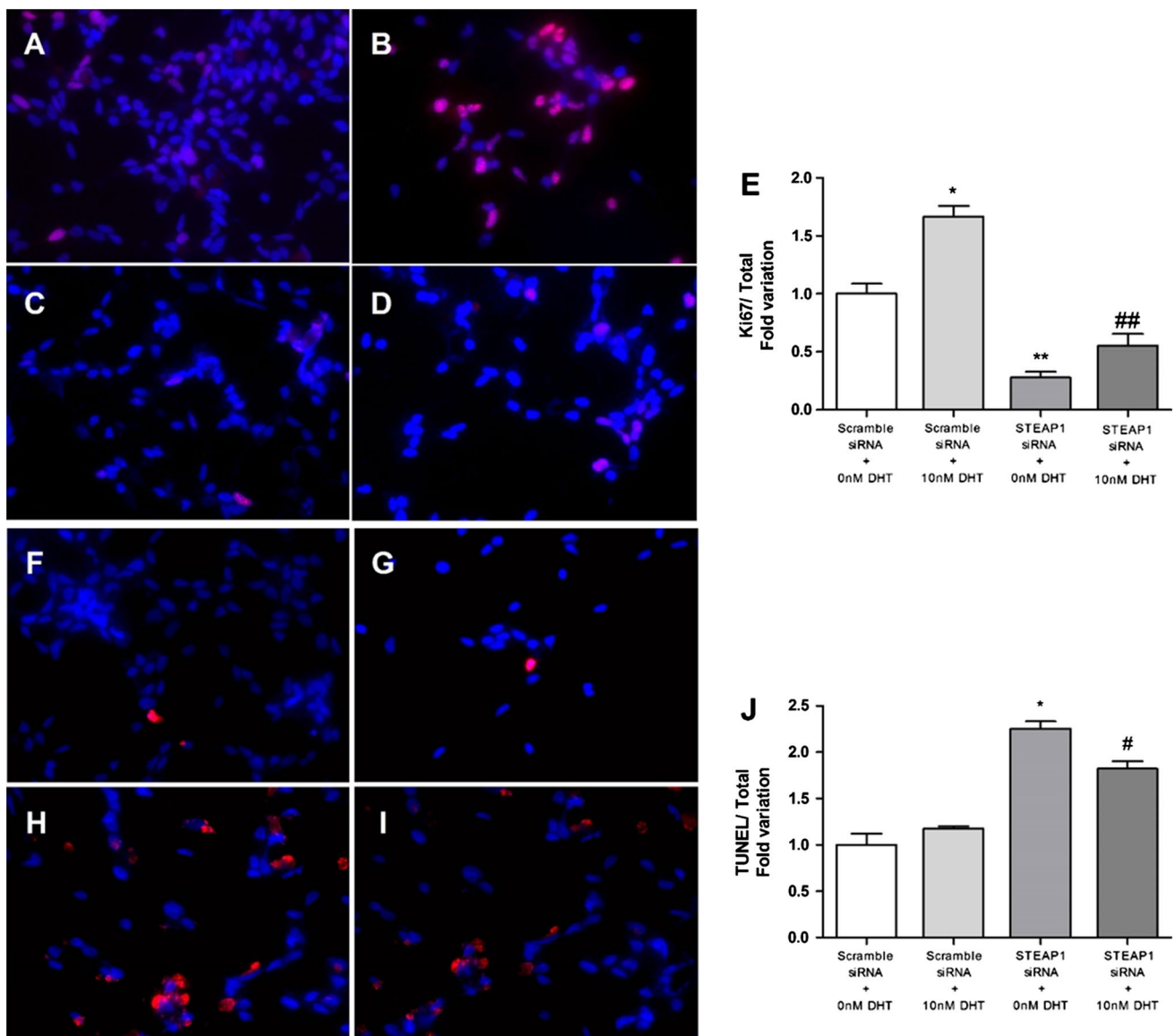**Fig. 3** Proliferation and apoptosis of LNCaP cells determined by Ki67 fluorescent immunocytochemistry (**a–e**) and using TUNEL assay (**f–j**), respectively. Representative images of merged Hoechst-stained nuclei, Ki67 and TUNEL immunofluorescence (×400 magnification) in scramble siRNA + 0 nM DHT (control, **a** and **f**), scramble siRNA + 10 nM DHT (**b, g**), STEAP1 siRNA + 0 nM DHT (**c, h**) and STEAP1 siRNA + 10 nM DHT (**d, i**) treated cells. Bar graphs indicate the percentage of Ki67 or TUNEL-positive cells relatively to total cells (**e, j**). Results are expressed as fold variation relatively to the control group. Error bars indicate mean ± SEM (*n* = 3). *$p < 0.05$, **$p < 0.01$ when compared to control; $^{##}p < 0.01$ when compared to scramble siRNA + 10 nM DHT-treated cells

variation relatively to control cells, $p < 0.001$ Fig. 4c). Regarding the intrinsic pathway of apoptosis, STEAP1 knockdown increased Bax protein expression by 1.5-fold relatively to control cells, $p < 0.01$, Fig. 5a, whereas the levels of the anti-apoptotic protein Bcl-2 levels remained unchanged (Fig. 5b); thereby, the Bax/Bcl-2 ratio was 2.0-fold increased ($p < 0.001$, Fig. 5c) in the STEAP1 knockdown cells in comparison with the control group. Considering that the increased Bax/Bcl-2 ratio may activate the initiator caspase-9, its expression was determined. STEAP1

knockdown increased the levels of caspase-9 when compared to control cells (1.4-fold variation, $p < 0.05$, Fig. 6b).

The extrinsic apoptosis pathway was also assessed by comparing the expression levels of FasR and FasL in experimental groups. After STEAP1 gene knockdown, a significant increase in FasL occurred (1.5-fold variation in comparison with control group, $p < 0.01$, Fig. 7b), but no statistical differences were observed in the expression of FasR (Fig. 7a). Caspase-8, which is activated by FasR, underwent a marked increase by STEAP1 knockdown in
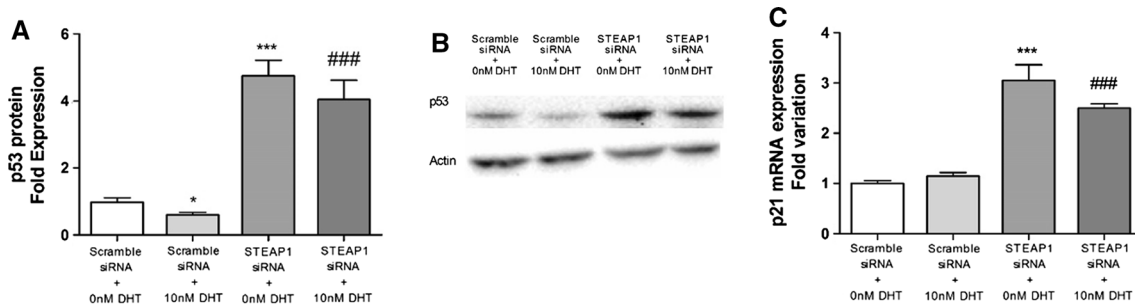
Fig. 4 Expression levels of the cell cycle regulators p53 (protein expression and representative immunoblots, **a** and **b,** respectively) and p21 (mRNA, **c**) in scramble siRNA + 0 nM DHT-treated cells (control), scramble siRNA + 10 nM DHT-treated cells, STEAP1 siRNA + 0 nM DHT-treated cells and STEAP1 siRNA + 10 nM DHT-treated cells. Results are expressed as fold variation relatively to the control group. Error bars indicate mean ± SEM ($n = 3$). *$p < 0.05$, ***$p < 0.001$ when compared to control; ###$p < 0.001$ when compared to scramble siRNA + 10 nM DHT-treated cells

Fig. 5 Protein expression levels of the apoptosis regulators Bax (**a**) and Bcl-2 (**b**) and Bax/Bcl-2 protein ratio (**c**) and representative immunoblots (**d**) in scramble siRNA + 0 nM DHT-treated cells (control), scramble siRNA + 10 nM DHT-treated cells, STEAP1 siRNA + 0 nM DHT-treated cells and STEAP1 siRNA + 10 nM DHT-treated cells. Results are expressed as fold variation relatively to the control group. Error bars indicate mean ± SEM ($n = 3$). *$p < 0.05$, **$p < 0.01$, ***$p < 0.001$ when compared to control; #$p < 0.05$, ###$p < 0.001$ when compared to scramble siRNA + 10 nM DHT-treated cells
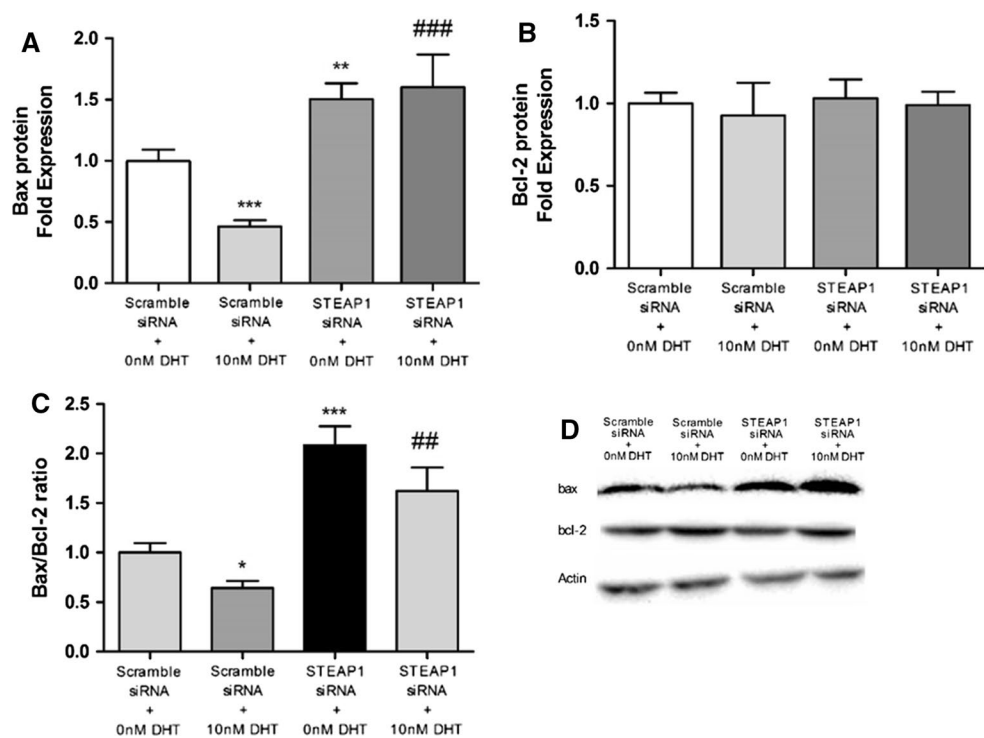
LNCaP cells compared to control cells (6.0-fold variation, $p < 0.01$, Fig. 6a).

Considering that caspase-3 is an effector of both pathways of apoptosis, its activity was also determined. Our results demonstrated that caspase-3 activity increased up to 2.3-fold variation ($p < 0.01$, Fig. 6d) in STEAP1 knockdown cells when compared to control cells.

The effect of DHT on LNCaP cells is abolished after STEAP1 gene knockdown

Considering that DHT is the main hormone responsible for prostate physiology and can be involved in the progression of PCa, we have evaluated whether the proliferative effects of DHT are abolished after STEAP1 gene silencing. As expected, the treatment of LNCaP cells with 10 nM DHT increased cell viability in 57 and 71% after 24 h and 48 h of treatment (Fig. 2, $p < 0.001$). The DHT-induced cell viability was significantly inhibited after STEAP1 gene silencing (46 and 60% reduction when compared to scramble siRNA + 10 nM DHT at 24 h or 48 h, respectively, $p < 0.001$). The effect of STEAP1 gene silencing alone is not reversed in the presence of 10 nM DHT.

Ki67 immunocytochemistry results showed a significant increase after treatment with DHT (1.7-fold variation relatively to control cells, Fig. 3a, b, e, $p < 0.05$). However,

Fig. 6 Protein expression levels of the apoptosis regulators caspase-8 (**a**) and caspase-9 (**b**), representative immunoblots (**c**) and caspase-3 activity (**d**) in scramble siRNA + 0 nM DHT-treated cells (control), scramble siRNA + 10 nM DHT-treated cells, STEAP1 siRNA + 0 nM DHT-treated cells and STEAP1 siRNA + 10 nM DHT-treated cells. Results are expressed as fold variation relatively to the control group. Error bars indicate mean ± SEM ($n = 3$). *$p < 0.05$, **$p < 0.01$, ***$p < 0.001$ when compared to control; #$p < 0.05$, ##$p < 0.01$, ###$p < 0.001$ when compared to scramble siRNA + 10 nM DHT-treated cells and $p < 0.05$ when compared to STEAP1 siRNA + 0 nM DHT-treated cells
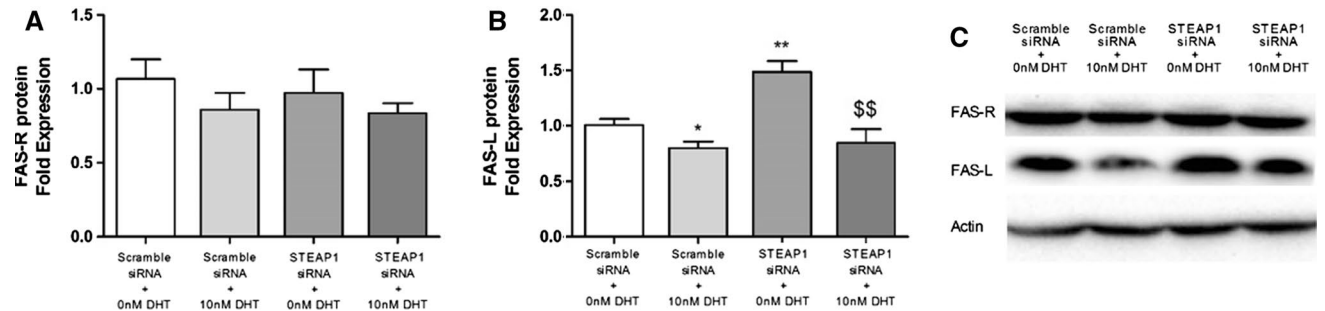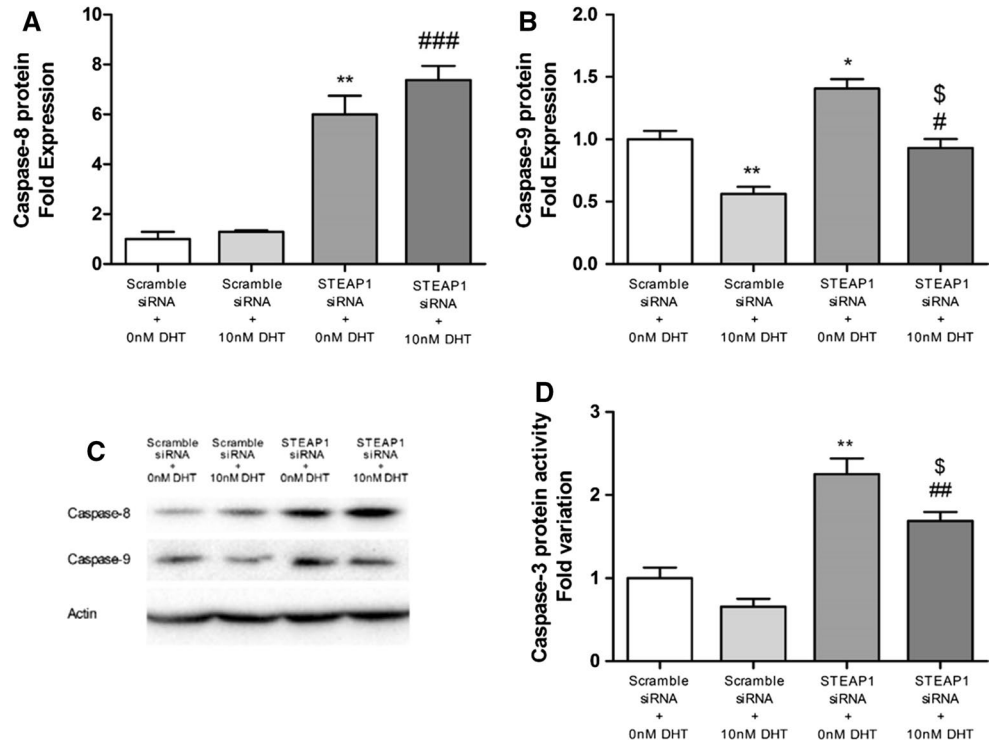
Fig. 7 Protein expression levels of the apoptosis regulators FasR (**a**), FasL (**b**) and representative immunoblots (**c**) in scramble siRNA + 0 nM DHT-treated cells (control), scramble siRNA + 10 nM DHT-treated cells, STEAP1 siRNA + 0 nM DHT-treated cells and STEAP1 siRNA + 10 nM DHT-treated cells. Results are expressed as fold variation relatively to the control group. Error bars indicate mean ± SEM ($n = 3$). *$p < 0.05$, **$p < 0.01$ when compared to control; and $p < 0.01$ when compared to STEAP1 siRNA + 0 nM DHT-treated cells

the positive effect of DHT was not observed in LNCaP cells knocked down for STEAP1 gene, where a significant reduction of Ki67-stained cells occurred (65% reduction in STEAP1 siRNA + 10 nM DHT when compared to scramble siRNA + 10 nM DHT, Fig. 3b, d, e, $p < 0.01$).

Concerning TUNEL assay, no effects were observed in LNCaP cells treated with 10 nM DHT when compared to control (scramble siRNA + 0 nM DHT) (Fig. 3f, g, j). The results also showed that the number of TUNEL-positive cells is significantly higher (60%) in STEAP1 knockdown + 10 nM DHT than in scramble siRNA + 10 nM DHT ($p < 0.05$, Fig. 3g, i, j).

Regarding the expression of cell cycle and apoptosis regulators, the treatment with DHT decreased the expression of p53 protein (0.6-fold variation relatively to control cells, $p < 0.05$, Fig. 4a, b). The increased expression of p53 induced by STEAP1 gene knockdown is not altered by the 10 nM DHT treatment. Also, the increased expression of p21 in LNCaP cells induced by the STEAP1 gene knockdown alone is not altered by DHT treatment ($p < 0.001$, Fig. 4c).

Regarding the intrinsic pathway of apoptosis, the results showed that Bax/Bcl-2 ratio decreases in LNCaP cells treated with DHT (0.6-fold variation when compared to scramble siRNA + 0 nM DHT) ($p < 0.05$, Fig. 5c), but not

in STEAP1 knockdown cells, where a significant increase in Bax/Bcl-2 ratio was observed (260% increase in STEAP1 siRNA + 10 nM DHT relatively to scramble siRNA + 10 nM DHT, $p < 0.01$). The expression of caspase-9 decreased in response to DHT treatment (0.6-fold variation relatively to control cells, $p < 0.01$, Fig. 6b), but its expression increased in STEAP1 knockdown cells treated with 10 nM DHT (40% increase when compared to scramble siRNA + 10 nM DHT, $p < 0.05$). However, the levels of caspase-9 are reduced in STEAP1 knockdown cells treated with 10 nM DHT when compared to STEAP1 siRNA + 0 nM DHT group (35% reduction, $p < 0.05$, Fig. 6b).

In what concerns the extrinsic apoptosis pathway, our results showed that the levels of FasL decreased in response to DHT treatment when compared to control group (0.8-fold variation, $p < 0.05$, Fig. 7b), and this effect is not changed by STEAP1 gene knockdown. Also, the STEAP1 knockdown-induced expression of FasL is abolished in the presence of DHT (45% reduction when compared to STEAP1 siRNA + 0 nM DHT, $p < 0.01$). On the other hand, the increased levels of caspase-8 in response to knockdown of STEAP1 gene are not abrogated by the treatment with DHT (Fig. 6a).

The activity of caspase-3 tends to decrease in response to DHT treatment when compared to control cells. However, a significant increase in caspase-3 activity was observed in STEAP1 knockdown cells treated with 10 nM DHT (125% increase when compared to scramble siRNA + 10 nM DHT, $p < 0.01$, Fig. 6d). On the other hand, the effect of STEAP1 knockdown alone is slightly reversed by DHT treatment (20% reduction in STEAP1 siRNA + 10 nM DHT relatively to STEAP1 siRNA + 0 nM DHT, $p < 0.05$, Fig. 6d).

Discussion

Apart from their complexity, most of cancers share a set of features that propel their progression. These include self-sufficient growth, apoptosis evasion, sustained angiogenesis, unlimited replicative potential, insensitivity to anti-growth signals and metastatic and invasion potential [21]. Understanding the mechanisms regulating PCa cellular proliferation and apoptosis provides a basis for identifying alternative targets for developing novel and more efficient therapies. STEAP1 is overexpressed in several types of cancer, including PCa [4–9]. To determine the role of STEAP1 in LNCaP cells viability, proliferation and apoptosis, we first induced STEAP1 gene knockdown by transfecting these cells with a specific siRNA against STEAP1 [22]. We confirmed that STEAP1 mRNA expression was reduced 24 h after transfection, while at protein level the reduction in STEAP1 levels was detected only after 24 and 48 h. The plausible cause for the time lapse required to repress protein expression may

be related to the transition period between transcription and translation and to the high stability of STEAP1 protein in LNCaP cells [23]. In an attempt to clarify the role of STEAP1 in the proliferation and apoptosis of LNCaP cells, we showed that STEAP1 knockdown significantly reduced LNCaP cells viability. Therefore, these results indicated that the inhibition of STEAP1 expression may decrease prostate cell growth and proliferation. Consistent with these observations, Ki67 immunofluorescence, a measure of the proliferation index, underwent a sharp reduction in STEAP1 knockdown cells. These results are supported by a previous report demonstrating that the blockage of STEAP1 using specific antibodies inhibits prostate tumor growth in vivo [17]. Data obtained with the TUNEL assay showed that the STEAP1 knockdown not only decreased cell proliferation but also increased the number of apoptotic cells. The reduced proliferation associated with increased apoptosis of LNCaP cells knocked down for the STEAP1 gene was accompanied by an altered expression of cell cycle regulators. It is well known that p53 and p21 pathways are involved in cell cycle arrest at G1 and S phases, as well as in induction of apoptosis [24–27]. Our results clearly evidenced that the activation of this pathway may be dependent on STEAP1 expression levels, considering the increased levels of p53 and p21 in LNCaP cells knocked down for STEAP1 when compared to controls. Furthermore, these observations stress the fact that the loss of STEAP1 expression leads to cell cycle arrest. Apoptosis is an essential and tightly regulated physiologic process that can be triggered by external or internal stimuli, activating extrinsic and intrinsic pathways, respectively. These pathways lead to the activation of initiator caspases, such as caspase-8 and caspase-9, respectively, and converge to the activation of caspase-3, an effector caspase, which is considered an end point of apoptosis and responsible for the majority of apoptotic events [28]. Analysis of caspase-3 activity evidenced that this protease is largely increased upon STEAP1 knockdown, an event that may be a consequence of extremely increased protein levels of caspase-8 and caspase-9. These results are supported by the increased Bax/Bcl-2 ratio and FasL in STEAP1 knockdown LNCaP cells. Considering that previous studies demonstrated that STEAP1 facilitates intracellular communication and intercellular transport in vivo, it is liable to speculate that the communication between LNCaP cells with STEAP1 knockdown might be compromised, and may stimulate the extrinsic and intrinsic pathway of apoptosis [17].

It is well documented that DHT is involved in tumor cell proliferation, either directly acting through its cognate receptor or by activating other signaling pathways [3, 29]. Considering that DHT regulates STEAP1 expression, we aimed to evaluate the effect of DHT in LNCaP cells with STEAP1 gene knockdown. Our results demonstrated that the positive effect of DHT in cell viability is

clearly blocked by STEAP1 gene silencing. In addition, DHT is not able to increase the cell viability in STEAP1-silenced cells, suggesting that DHT cannot reverse the effects of STEAP1 knockdown and the DHT effect seems to be dependent on STEAP1 levels in LNCaP cells. These results are also supported by the determination of Ki67 index, where the effect of DHT is abolished in LNCaP cells knocked down for STEAP1 gene. Therefore, these results emphasize that the STEAP1 knockdown may have a repressive effect on DHT action in PCa.

Moreover, the obtained results are also supported by the TUNEL assays and the expression of apoptosis regulators such as p53, Bax/Bcl-2 ratio and caspase-3, caspase-8 and caspase-9. Overall, the treatment with DHT can reverse the effect of STEAP1 knockdown in caspase-9 expression and caspase-3 activity, but even so, their levels are higher when compared to scramble siRNA + DHT. Taken together, these results suggested that STEAP1 overexpression is not only involved in cell proliferation and apoptosis but also may favor the proliferative and anti-apoptotic effects of DHT in LNCaP cells. Although more studies are required, our results suggested that targeting STEAP1 protein may turn cancer cells more susceptible to apoptosis. In addition, it is liable to speculate that blocking STEAP1 protein may be a good strategy to prevent the proliferative effects of DHT in cancer cells.

In conclusion, our study demonstrated that STEAP1 gene knockdown promoted apoptosis mediated by either extrinsic or intrinsic pathway. In addition, it decreased cell proliferation and prevented the proliferative and anti-apoptotic effects of DHT in LNCaP cells, strengthening the idea that STEAP1 is a very promising therapeutic target against hormone-dependent PCa.

Compliance with ethical standards

Conflict of interest The authors declare that they have no conflicts of interest with the contents of this article.

Ethical approval This article does not contain any studies with human participants or animals performed by any of the authors.

References

1. Siegel RL, Miller KD, Jemal A. Cancer statistics, 2016. CA Cancer J Clin. 2016;66(1):7–30.
2. de Marzo AM, et al. Stem cell features of benign and malignant prostate epithelial cells. J Urol. 1998;160(6):2381–92.
3. Wang D, Tindall DJ. Androgen action during prostate carcinogenesis. In: Saatcioglu F, editor. Androgen action. Berlin: Springer; 2011. p. 25–44.
4. Grunewald TG, et al. STEAP1 is associated with the invasive and oxidative stress phenotype of Ewing tumors. Mol Cancer Res. 2012;10(1):52–65.
5. Hubert RS, et al. STEAP: a prostate-specific cell-surface antigen highly expressed in human prostate tumors. PNAS. 1999;96(25):14523–8.
6. Maia CJB, et al. STEAP1 is over-expressed in breast cancer and down-regulated by 17beta-estradiol in MCF-7 cells and in the rat mammary gland. Endocrine. 2008;34(1–3):108–16.
7. Yang D, et al. Murine six-transmembrane epithelial antigen of the prostate, prostate stem cell antigen, and prostate-specific membrane antigen: prostate-specific cell-surface antigens highly expressed in prostate cancer of transgenic adenocarcinoma mouse prostate mice. Cancer Res. 2001;61(15):5857–60.
8. Gomes IM, et al. Six transmembrane epithelial antigen of the prostate 1 is down-regulated by sex hormones in prostate cells. Prostate. 2012;73(6):605–13.
9. Gomes IM, Arinto P, Lopes C, Santos CR, Maia CJ. STEAP1 is over-expressed in prostate cancer and prostatic intraepithelial neoplasia lesions, and it is positively associated with Gleason score. Urol Oncol Semin Orig Investig. 2013;32(1):53.e23–9.
10. Barroca-Ferreira J, et al. Targeting STEAP1 protein in human cancer: current trends and future challenges. Curr Cancer Drug Targets. 2018;18(3):222–30. https://doi.org/10.2174/1568009617666170427103732.
11. Alves PMS, et al. STEAP, a prostate tumor antigen, is a target of human CD8+ T cells. Cancer Immunol Immun. 2006;55(12):1515–23.
12. Azumi M, et al. Six-transmembrane epithelial antigen of the prostate as an immunotherapeutic target for renal cell and bladder cancer. J Urol. 2010;183(5):2036–44.
13. Garcia-Hernandez MDLL, et al. In vivo effects of vaccination with six-transmembrane epithelial antigen of the prostate: a candidate antigen for treating prostate cancer. Cancer Res. 2007;67(3):1344–51.
14. Grunewald T, et al. High STEAP1 expression is associated with improved outcome of Ewing's sarcoma patients. Ann Oncol. 2012;23(8):2185–90.
15. Valenti MT, et al. STEAP mRNA detection in serum of patients with solid tumours. Cancer Lett. 2009;273(1):122–6.
16. Gomes IM, Maia CJ, Santos CR. STEAP proteins: from structure to applications in cancer therapy. Mol Cancer Res. 2012;10(5):573–87.
17. Challita-Eid PM, et al. Monoclonal antibodies to six-transmembrane epithelial antigen of the prostate-1 inhibit intercellular

communication in vitro and growth of human tumor xenografts in vivo. Cancer Res. 2007;67(12):5798–805.

18. Yamamoto T, et al. Six-transmembrane epithelial antigen of the prostate-1 plays a role for in vivo tumor growth via intercellular communication. Exp Cell Res. 2013;319(17):2617–26.

19. Valenti M, et al. Zoledronic acid decreases mRNA six-transmembrane epithelial antigen of prostate protein expression in prostate cancer cells. J Endocrinol Invest. 2010;33(4):244–9.

20. Pfaffl MW. A new mathematical model for relative quantification in real-time RT-PCR. Nucleic Acids Res. 2001;29(9):e45.

21. Hanahan D, Weinberg RA. The hallmarks of cancer. Cell. 2000;100(1):57–70.

22. Carthew RW, Sontheimer EJ. Origins and mechanisms of miRNAs and siRNAs. Cell. 2009;136(4):642–55.

23. Gomes IM, Santos CR, Maia CJ. Expression of STEAP1 and STEAP1B in prostate cell lines, and the putative regulation of STEAP1 by post-transcriptional and post-translational mechanisms. Genes Cancer. 2014;5(3–4):142–51.

24. He G, et al. Induction of p21 by p53 following DNA damage inhibits both Cdk4 and Cdk2 activities. Oncogene. 2005;24(18):2929–43.

25. Pietenpol JA, Stewart ZA. Cell cycle checkpoint signaling: cell cycle arrest versus apoptosis. Toxicology. 2002;181–182:475–81.

26. Gan L, et al. Resistance to docetaxel-induced apoptosis in prostate cancer cells by p38/p53/p21 signaling. Prostate. 2011;71(11):1158–66.

27. Abbas T, Dutta A. p21 in cancer: intricate networks and multiple activities. Nat Rev Cancer. 2009;9(6):400–14.

28. Zimmermann KC, Green DR. How cells die: apoptosis pathways. J Allergy Clin Immunol. 2001;108(4, Supplement):S99–103.

29. Lee C, et al. Regulation of proliferation and production of prostate-specific antigen in androgen-sensitive prostatic cancer cells, LNCaP, by dihydrotestosterone. Endocrinology. 1995;136(2):796–803.